Role of Core Interactions and External Perturbations in the Autoionization of Xe

Marc J. J. Vrakking

FOM Institute for Atomic and Molecular Physics (AMOLF), Kruislaan 407, 1098 SJ Amsterdam, The Netherlands

Received: February 28, 1997; In Final Form: May 28, 1997[⊗]

In a recent paper (Vrakking, M. J. J.; Lee, Y. T.; *J. Chem. Phys.* **1995**, *102*, 8833) we reported that autoionization rates of Xe Rydberg states converging on the $^2P_{1/2}$ upper spin orbit state of Xe^+ strongly depend on the presence of dc electric fields and surrounding ions. In the current paper, we present theoretical calculations that illustrate that the observed electric field dependence of the autoionization rates is influenced by the existence of short-range Rydberg electron−core interactions. In the presence of dc electric fields the autoionization rates decrease as a result of orbital angular momentum mixing. In the case of the ns′$[1/2]_1$ series, mixing with the high-*l* manifold is mediated by short-range interactions with the rapidly autoionizing nd′$[3/2]_1$ series. As a result, effective *l*-mixing takes place at substantially lower electric field strengths than would otherwise be the case. The experimental results of the dc electric field dependence of Xe pulsed field ionization (PFI) signals are compared with the theory, and predictions are made for sub-nanosecond time-resolved ionization experiments.

Introduction

While preparing to write this paper, I looked up a fax message that I received from Yuan Lee in February of 1994. At that time he had just assumed his current position as president of the Academia Sinica in Taiwan, and in Berkeley preparations were under way for a series of experiments on Rydberg states of the NO molecule. It was eventful time: one week there was the infamous "sprinkler incident", which brought the Berkeley fire department out in force, and in the following week the first experimental results were obtained, which, of course, I sent to Yuan immediately. The answer, by fax, was typical Yuan: "I was glad to learn that the excitement caused by the 'stream of water' has now turned into a stream of scientific results!".

The experimental results that Yuan was referring to were measurements of the lifetimes of high-*n* predissociating Rydberg states of the NO molecule and the way these lifetimes can be manipulated by the application of a small dc electric field.[1,2] Lifetimes of high-*n* Rydberg states have attracted considerable attention in recent years, as a result of observations in zero-kinetic-energy photoelectron spectroscopy (ZEKE) experiments. ZEKE is a spectroscopic technique where electrons are collected that are formed by pulsed field ionization (PFI) of high-*n* Rydberg states. Because small ionization fields are used, electrons are only obtained from Rydberg states very close to the convergence limit of a Rydberg series (typically $n \approx 150-200$), and therefore ZEKE allows the determination of ionization thresholds at laser-limited resolution. An essential component of a ZEKE experiment is that there is a time delay between the laser excitation and the PFI. During this time delay prompt electrons formed by the excitation laser(s) are removed using a small (stray) dc field. Remarkably, many examples now exist where ZEKE spectra have been recorded at pulsed field delay times far exceeding the anticipated lifetime of the high-*n* Rydberg states. Rydberg states are nice model systems for dynamical studies, since many of their properties (positions of the energy levels and level spacings, decay parameters, etc.) are described by simple scaling laws. Therefore, a measurement of the natural linewidth of an $n = 10$ Rydberg state should typically allow one to predict with reasonable accuracy the linewidth (and lifetime) for $n = 150-200$, by using an n^3 scaling law. Rydberg states in ZEKE experiments frequently violate the simple scaling laws.

The deviations of high-*n* Rydberg lifetimes from simple scaling behavior have been explained in terms of a number of models, which rationalize the observed lifetime enhancements either as the effect of intramolecular couplings and/or as the result of external perturbations. Levine and co-workers have emphasized the importance of intramolecular couplings, which bring the Rydberg state which is optically excited in contact with a "bath" of surrounding states.[3,4] If the decay of the Rydberg population is intimately connected with the decay of the initially populated state, then coupling to the background states can lead to a lifetime enhancement. For example, if the initially excited state is a low-*J* rotational state that decays predominantly via autoionization, then coupling to higher-*J* (and lower *n*) Rydberg states—which cannot autoionize directly—can lead to a lifetime enhancement.[5,6] Discussions about the applicability of this model have especially centered on the question of possible decay channels of the background states (i.e. by routes other than the low-*J* autoionization process).[7]

The idea of enhancement of Rydberg lifetimes in ZEKE through external perturbations was first put forward by Chupka, who argued that the enhanced Rydberg lifetimes might be the result of small dc electric fields and/or interactions with surrounding ions.[8] In the presence of a dc electric field the orbital angular momentum of a Rydberg electron is no longer conserved. In the angular momentum basis, the Rydberg electron performs a periodic oscillation between the initially prepared low-*l* state and a high-*l* state.[9] Whenever the expectation value of the orbital angular momentum is large, the interaction of the electron with the ionic core is turned off. At these times, decay channels like autoionization and predissociation, which can be looked upon as a "reactive" collision between the Rydberg electron and the ionic core (in which energy is exchanged between the Rydberg electron and the rovibrational and/or electronic degrees of freedom of the ionic core), cease to exist. A lifetime enhancement can thus occur,

[⊗] Abstract published in *Advance ACS Abstracts,* August 1, 1997.

S1089-5639(97)00756-1 CCC: $14.00

since the field reduces the frequency of interaction between the ionic core and the Rydberg electron[10] (a "stretching of the time-axis"[11]).

In similar fashion, interactions with surrounding ions can alter the lifetime. If the Rydberg atom/molecule is produced in an environment where it is surrounded by ions, then the total electric field experienced by the Rydberg atom/molecule will be both inhomogeneous and time-dependent. The field inhomogeneity is due to the fact that the total dc electric field experienced by the Rydberg electron varies over the orbit of the Rydberg electron. At the same time, both the magnitude and the direction of the total field change as the Rydberg atom/molecule and the ion(s) move with respect to each other. The importance of both effects has been advocated in the literature.[12,13] In inhomogenous or time-dependent electric fields the projection of the angular momentum onto the field axis (which is a conserved quantity in a constant homogeneous dc electric field) will no longer be conserved. In the angular momentum basis, the electron propagates both in the orbital angular momentum l and in the projection quantum number m, which, due to the $(2l+1)$-fold m-degeneracy of the l-states, leads to a further reduction of the fraction of time spent at low angular momentum.

Chupka's paper prompted us to investigate the lifetimes of predissociating Rydberg states of the NO molecule[1,2] and autoionizing Rydberg states of the Xe atom.[14] A near-transform-limited pulsed dye laser ($\Delta\omega \leq 0.005$ cm^{-1}) was used to excite individual high-n Rydberg states of NO and Xe, and the lifetimes of these Rydberg states were determined by measuring the NO^+ signal, and, in the case of Xe, the pulsed field electron signal, as a function of the time delay between the laser excitation and the pulsed field ionization. The results provided clear evidence for both of the mechanisms proposed by Chupka. In the NO experiment, a sudden increase in the lifetimes of p- and f-orbital Rydberg states was observed as a function of the principal quantum number, which could be attributed to the presence of a small dc stray electric field in the apparatus (estimated at 25 mV/cm). In the case of Rydberg states that did not undergo a lifetime enhancement as a result of the stray field ($n < 65$ in case of the f-series and $n < 116$ in case of the p-series), the lifetimes could readily be enhanced through the application of a dc field *in excess* of the stray field. In the Xe experiments, the pulsed field ionization (PFI) signals could similarly be manipulated by the application of dc electric fields. Furthermore it was found that the PFI signal had a near-quadratic dependence on the Xe pressure. Combined with the observed laser power dependence of the PFI signal, this observation provided considerable support for the mechanism of ion-enhanced Rydberg lifetimes.

Similar observations have been reported by a number of other authors. Prior to our experiments, Pratt performed a study on the NO molecule, where he observed a lifetime reduction when applying a dc field, as well as an overall lifetime enhancement which he attributed to the presence of ions.[15] In this study, the effect of a dc electric field was studied at somewhat larger field strengths, and the observation of a lifetime reduction is consistent with our lifetime enhancement at lower field strengths.[2] Merkt studied the role of dc electric fields and collisional effects in autoionizing Rydberg states of Ar. He observed a lifetime enhancement over the natural lifetimes, which he attributed to ion−Rydberg interactions and an inhibition of the formation of long-lived Rydberg states in the presence of dc fields, due to the fact that efficient l,m-mixing requires a near-degeneracy among the interacting levels, which is broken by the dc field.[16,17] In recent experiments on NO, using a sequence of field ionization pulses, he obtained direct evidence for the existence of this requirement.[18]

Rydberg states of the benzene molecule were studied, at high resolution, by Neuhauser and Neusser.[19,20] At dc field strengths between 50 and 300 mV/cm they observed enhanced lifetimes which they attributed to l-mixing of the near-zero quantum defect optically accessed states. Schlag and co-workers observed that benzene ZEKE signals were greatly reduced when dc electric fields over 200 mV/cm were applied, although the lifetimes of the Rydberg states that are eventually detected in the experiment (after a time delay of a few tens of microseconds) *increased* when a field was present during the time delay between the excitation and the pulsed field ionization.[21] As in the case of NO, these observations illustrate that the effect of a dc electric field need not be monotonous, but can vary, as more and more low-l states merge into the Stark manifold.

Regarding ion−Rydberg interactions, Schlag et al. observed a disappearance of the benzene PFI signals when the total ion yield was extrapolated to zero.[12,22] At the same time they observed evidence for saturation of the influence of ion−Rydberg interactions: in an earlier study on the lifetimes of the C_6H_6 Rydberg states they observed no effect when varying the density of $C_6D_6^+$ ions,[23] since complete l,m-randomization occurred as a result of the production of $C_6H_6^+$, concurrent with the Rydberg excitation step. In this context, it is interesting to mention also two recent experiments on the lifetimes of spin−orbit autoionizing Rydberg states of Ar. While Hepburn and co-workers found evidence for stabilization of Rydberg states by surrounding ions in a low-repetition rate laser experiment (where a significant number of ions can be produced),[24] Hsu et al., in a quasi-CW experiment at the Chemical Dynamics Beamline of the Advanced Light Source (under conditions where surrounding ions are absent), were unable to obtain any pulsed field ionization signals.[25]

Besides a better understanding of the Rydberg dynamics pertaining to ZEKE experiments, studies of the lifetime dynamics of high-n atomic and molecular Rydberg states have now started producing interesting experimental spinoffs. Zare and co-workers utilized the fact that H_2 Rydberg states can be stabilized through interactions with surrounding ions to produce long-lived ($\tau \geq 20$ μs) Rydberg states, which were used in high-resolution time-of-flight measurements of the products a bimolecular chemical reaction.[26,27] In femtosecond vibrational wavepacket experiments on the I_2 molecule we used the fact that I_2 Rydberg states can be stabilized by surrounding ions to create a "ZEKE amplifier".[28]

In a recent paper we presented a theoretical analysis of the dc electric field induced lifetime enhancement of predissociating Rydberg states of NO.[29] This work was motivated by our experimental observation that the onset for lifetime enhancement in the NO molecule was extremely sudden. Specifically, for the p-series converging on $N^+ = 0$, we observed that under experimental conditions of dc stray electric fields only, the 115p level had a lifetime close to its natural lifetime (7.1 ± 1.6 ns), whereas the neighboring 116p level displayed an approximately 15-fold lifetime enhancement (114 ± 27 ns). Our analysis showed that the suddenness of the onset of the lifetime enhancement was a manifestation of the multiexponential nature of the decay of the initially prepared state. The presence of an electric field leads to a dilution of the low-l character, which provides the doorway to excitation, among a number of Stark states. Variations in the lifetimes of these individual Stark states then lead to a multiexponential decay of the Rydberg population. The interpretation of experimental results therefore requires a careful assessment of the ability of the experiment to distinguish

and/or detect with equal sensitivity a range of different lifetimes. The importance of the multiexponential nature of the decay of the initially prepared Rydberg population was also emphasized by Bixon and Jortner[30,31] and, recently, by Lefebvre-Brion and collaborators.[32]

In our theoretical NO paper, we developed a Hamiltonian description of the NO molecule, which was based on an adaptation of earlier results obtained by multichannel quantum defect theory (MQDT).[33,34] The results of an MQDT analysis by Fredin et al. were used to set up a Hamiltonian describing the coupling among Hund's case d basis states induced by short-range Rydberg electron−core interactions.[35] These computations complemented work by Bixon and Jortner, who analyzed the role of long-range dipolar Rydberg electron−core interactions and concluded that in NO these interactions play a negligible role, except for a few isolated instances where near-resonances occur.[36] In our work we considered two kinds of short range core interactions. First of all, interactions were considered where for a given l different core rotational states are coupled. These couplings describe Rydberg electron−core collisions, where a low-l Rydberg electron penetrates the ionic core, so that a Hund's case d description ceases to be valid (i.e. the core rotational quantum number is no longer well-defined). When the Rydberg electron re-emerges from the core, the core rotational state becomes well-defined again, but now the core rotational state may no longer be the same as prior to the collision. Put differently, there is a coupling between different core rotational states. Secondly, interactions were considered where different low-l angular momentum states are coupled through close-range interactions with the core. In particular, the mixing of sσ and dσ configurations was considered. In this case, an s- or d-electron penetrates the ionic core, where the orbital angular momentum is only characterized by its projection (σ) onto the internuclear axis. Now, when the Rydberg electron re-emerges from the core region, both the core rotational state and the orbital angular momentum of the Rydberg electron may have undergone a change; in other words, there is a coupling between s- and d-orbital Rydberg series converging on a range of rotational states.

While in the case of NO we could reproduce the gross features of the experimental lifetime enhancements without including the short-range interactions, a comparison of the theoretical results with and without inclusion of the short-range core interactions nevertheless illustrated the way in which these interactions are operative in the principal quantum number range of interest. Efforts are currently under way to extend these calculations to the regime around $n = 200$, where the ZEKE experiments are actually performed.

In this paper we show how short-range core interactions also play an important role in the autoionization experiments on the Xe atom.[14] Experimentally, we investigated the lifetimes of $n = 40-80$ Rydberg states of the Xe atom, using either the ns′-$[1/2]_1$ or nd′$[3/2]_1$ Rydberg series as doorway state. The experimental observation that both the application of a dc electric field and ion densities on the order of 10^5-10^7 cm^{-3} were necessary in order to obtain a measurable PFI signal suggested the following scenario for the lifetime enhancement. First, the application of a dc electric field leads to (rapid) l-mixing and an enhancement of the lifetime from sub-nanosecond to a few nanoseconds. Secondly, the presence of ions around the Rydberg atoms leads to an evolution in the magnetic quantum number m and an additional lifetime enhancement to a few tens of nanoseconds. In the current paper, we specifically focus on the initial stage of the lifetime enhancement, i.e. the l-mixing introduced by the presence of a dc electric field. Since the coupling induced by the electric field is dipolar, we would anticipate a hierarchical onset for the coupling of the low-l Rydberg series to the Stark manifold containing the high-l states. In other words, lifetime alterations of the nd′$[3/2]_1$ state through mixing with the high-l manifold ought to precede mixing of the ns′$[1/2]_1$ state. Indeed, this is what was observed by Softley and co-workers in a recent MQDT computation of the Stark effect in autoionizing Rydberg states of Ar.[37] Nevertheless, our experimental observation in Xe was that the onset for lifetime enhancement of the ns′$[1/2]_1$ series came at significantly lower dc electric field strengths than the nd′$[3/2]_1$ series. We will demonstrate that the "premature" mixing of the ns′$[1/2]_1$ series with the high-l manifold is a manifestation of the presence of Rydberg electron−core mixing. As a result of this mixing the ns′$[1/2]_1$ series acquires some nd′ character even at zero dc electric field, which allows mixing of this state with the high-l manifold as soon as the ns′$[1/2]_1$ state crosses the Stark manifold. Since we calculate only the l-mixing by the dc field and not the m-mixing due to the presence of surrounding ions, the lifetimes that we will calculate necessarily differ from the experimentally observed decay times. However, the dependence of the PFI signals on the presence of a dc electric field ought to be rather similar in experiments with or without surrounding ions, and thus the conclusions reached about the role of Rydberg electron−core interactions which are presented are applicable to the previously reported experiments.

Theory

(a) Description of the Hamiltonian. The theoretical approach utilized in this paper is similar to the one used in our recent paper on dc electric field induced lifetime enhancement of high-n predissociating Rydberg states of the NO molecule.[29] Therefore, only a brief description will be presented here. Similar to earlier treatments of Xe autoionization by Knight and Wang[38] and Ernst et al.,[39] the calculations are based on diagonalization of the Stark Hamiltonian which describes the coupling between jl-coupled basis states, which are expressed as $nl[K]_J$. Here, n and l have the usual meaning of principal quantum number and orbital angular momentum of the Rydberg electron. The angular momentum j of the $^2P_{1/2}$ ionic core combines with l to form a resultant angular momentum K, which then couples with the Rydberg electron spin s to form J. Following diagonalization of the Hamiltonian, the eigenvalues of the Stark states are obtained, as well as the eigenvectors expressed in terms of the field-free basis states. On the basis of known decay rates of the field-free states, individual decay widths of the Stark states are determined, which allow the evaluation of a number of time-dependent observables.

Our calculation differs from the methodology of Bixon and Jortner, who included the decay width of the field-free basis states as a complex diagonal component in the Stark Hamiltonian in their work on autoionization in Ar[40] and predissociation in NO.[41] They thereby obtained the lifetimes of the Stark states directly in the diagonalization. Ideally our approach would be replaced by a full effective Hamiltonian treatment, in which both diagonal and off-diagonal complex matrix elements are included. However, evaluation of the off-diagonal matix elements requires an ab-initio calculation. In principle, the preferred method to analyze the structure and dynamics of Stark manifolds is multichannel quantum defect theory (MQDT). This method was recently applied by Softley and co-workers to the autoionization of Ar, N_2, and H_2.[37] A disadvantage discussed by Softley et al. is that the evaluation of the Stark excitation spectrum at a *single* electric field strength requires the diagonalization of hundreds of large (typically 250 × 250, for the

Chart 1

	s′(1/2)$_0$	s′(1/2)$_1$	p′(1/2)$_0$	p′(1/2)$_1$	p′(3/2)$_1$	p′(3/2)$_2$	d′(3/2)$_1$	d′(3/2)$_2$	d′(5/2)$_2$	d′(5/2)$_3$	f′(5/2)$_2$	f′(5/2)$_3$	f′(7/2)$_3$	f′(7/2)$_4$
s′(1/2)$_0$	H_{el}			H_F	H_F									
s′(1/2)$_1$		H_{el}	H_F			H_F	$H_{s'd'}$							
p′(1/2)$_0$		H_F	H_{el}				H_F							
p′(1/2)$_1$	H_F			H_{el}				H_F						
p′(3/2)$_1$	H_F				H_{el}			H_F	H_F					
p′(3/2)$_2$		H_F				H_{el}	H_F			H_F				
d′(3/2)$_1$		$H_{s'd'}$	H_F			H_F	H_{el}				H_F			
d′(3/2)$_2$				H_F	H_F			H_{el}				H_F		
d′(5/2)$_2$					H_F				H_{el}			H_F	H_F	
d′(5/2)$_3$						H_F				H_{el}				H_F
f′(5/2)$_2$							H_F				H_{el}			
f′(5/2)$_3$								H_F	H_F			H_{el}		
f′(7/2)$_3$									H_F				H_{el}	
f′(7/2)$_4$										H_F				H_{el}

situations described in the current paper) complex matrices. In our current paper, dynamical variables of the Stark states were calculated at as many as 500 different electric field strengths. In this situation an MQDT calculation would appear to be prohibitive.

The Hamiltonian, which is shown schematically in (Chart 1), contains three kinds of terms: (i) the zero-order electronic energies H_{el}, (ii) coupling matrix elements due to the presence of a dc electric field H_F, and (iii) coupling matrix elements due to short-range Rydberg electron−core interactions $H_{s'd'}$.

The zero-order electronic energies H_{el} follow from experimentally observed quantum defects as

$$H_{el} = -\mu_{lKJ}/\nu^3 \qquad (2)$$

where μ_{lKJ} is the quantum defect and $\nu = n - \mu_{lKJ}$ is the effective principal quantum number. A summary of the quantum defects used in the calculations is given in Table 1. Quantum defects for the ns′$[1/2]_0$, the nd′$[3/2]_2$, the nd′$[5/2]_2$, and the nd′$[5/2]_3$ series were taken from Wang and Knight,[42] whereas the quantum defects of the np′$[1/2]_0$, the np′$[1/2]_1$, the np′$[3/2]_1$, the np′$[3/2]_2$, and the nf′ series were taken from Ernst et al.[39] For the ns′$[1/2]_1$ and nd′$[3/2]_1$ series we used quantum defects derived from our own experiments, and for $l > 3$ all quantum defects were set to zero.

According to the pioneering MQDT analysis of Lu,[43] the ns′-$[1/2]_1$ and nd′$[3/2]_1$ configurations are coupled as a result of core penetration. Therefore the diagonal matrix elements for these configurations are altered to

$$H_{ns,n's} = -(\cos^2\theta\,\mu_{s,0} + \sin^2\theta\,\mu_{d,0})/(\nu_n^{3/2}\,\nu_{n'}^{3/2})$$

$$H_{nd,n'd} = -(\sin^2\theta\,\mu_{s,0} + \cos^2\theta\,\mu_{d,0})/(\nu_n^{3/2}\,\nu_{n'}^{3/2}) \qquad (3)$$

where θ is the mixing angle between the ns′$[1/2]_1$ and nd′$[3/2]_1$ configurations.

Lu estimated the mixing angle to be approximately 0.15 radians. Core penetration of the ns′ and the nd′ Rydberg electrons also leads to off-diagonal coupling matrix elements $H_{ns,n'd}$ between the ns′$[1/2]_1$ and nd′$[3/2]_1$ series, which are given by[14]

$$H_{ns,n'd} = {}^1/_2\sin 2\theta(\mu_{s,0} - \mu_{d,0})/(\nu_n^{3/2}\nu_{n'}^{3/2}) = -\mu_{s'd'}(\theta)/(\nu_n^{3/2}\nu_{n'}^{3/2}) \qquad (4)$$

In our calculations we specifically wanted to investigate the role of the mixing angle θ, and therefore θ is treated here as a parameter that is not known a priori. As a result, θ-dependent $\mu_{s,0}$ and $\mu_{d,0}$ quantum defects had to be used, which were chosen such that the experimental eigenenergies of the ns′$[1/2]_1$ and nd′$[3/2]_1$ series are recovered when the field-free Hamiltonian is diagonalized. From a prediagonalization of a field-free (2 × 2) Hamiltonian with basis states ns′$[1/2]_1$ and nd′$[3/2]_1$, it follows that the eigenvalues of the ns′$[1/2]_1$ and nd′$[3/2]_1$ series are independent of the coupling matrix element $H_{ns',nd'}$ when $\mu_{s,0}$ and $\mu_{d,0}$ are chosen according to:

$$\mu_{s,0}(\theta) = \mu_{s'} + \Delta$$

$$\mu_{d,0}(\theta) = \mu_{d'} - \Delta \qquad (5)$$

where

$$\Delta = {}^1/_2\{(\mu_{d'} - \mu_{s'}) + [(\mu_{d'} - \mu_{s'})^2 - 4\mu_{s'd'}(\theta)]^{1/2}\} \qquad (6)$$

where $\mu_{s'}$ and $\mu_{d'}$ are the experimentally observed quantum defects of the ns′$[1/2]_1$ and nd′$[3/2]_1$ series. Similarly, θ-dependent autoionization rates $\Gamma_{ns'[1/2]_1}$ and $\Gamma_{ns'[1/2]_1}$ were used to ensure that the calculated autoionization rates at zero electric field correspond to the experimentally observed autoionization rates.

The electric field couples different Rydberg series subject to the selection rules $\Delta J = \pm 1$, $\Delta l = \pm 1$, and $\Delta K = 0, \pm 1$. The matrix elements due to the presence of the field are given by

$$H_F[lKJ,l'K'J'] = -eF\langle\nu lKJ|z|\nu'l'K'J'\rangle = -eF(-1)^{K+K'+J+J'+l+j+S}[(2K+1)(2K'+1)(2J+1)\times(2J'+1)]^{1/2}\begin{bmatrix} J & 1 & J' \\ 0 & 0 & 0 \end{bmatrix}\begin{Bmatrix} K & J & S \\ J' & K' & 1 \end{Bmatrix}\begin{Bmatrix} l & K & j \\ K' & l' & 1 \end{Bmatrix}\langle\nu\|r\|\nu'l'\rangle \qquad (7)$$

where

TABLE 1: Quantum Defects and Decay Rates of the Zero-Order States

state	quantum defect [ref]	decay width Γ_0 (cm^{-1}) [ref]
ns′$[1/2]_0$	4.021 [42]	1400 [42]
ns′$[1/2]_1$	4.010 [14]	1300 [42]
np′$[1/2]_0$	3.500 [39]	500[a]
np′$[1/2]_1$	3.548 [39]	500[a]
np′$[3/2]_1$	3.581 [39]	500[a]
np′$[3/2]_1$	3.560 [39]	500[a]
nd′$[3/2]_1$	2.320 [14]	35000 [42]
nd′$[3/2]_2$	2.451 [42]	12000 [42]
nd′$[5/2]_2$	2.474 [42]	4000 [42]
nd′$[5/2]_3$	2.435 [42]	6000 [42]
nf′$[5/2]_2$	0.055 [39]	200[a]
nf′$[5/2]_3$	0.055 [39]	200[a]
nf′$[7/2]_3$	0.055 [39]	200[a]
nf′$[7/2]_4$	0.055 [39]	200[a]
nl′(l>3)	0.000	50[a]

[a] The linewidths of the np′, the nf′, and the n(l>3) are not known. Values listed have been used in the computations.

$$\langle \nu l \| r \| \nu' l' \rangle = -(l+1)^{1/2} \langle \nu l | r | \nu' l+1 \rangle \qquad l' = l+1$$
$$l^{1/2} \langle \nu l | r | \nu' l-1 \rangle \qquad l' = l-1 \quad (8)$$

The radial integrals were evaluated using the results of Edmonds et al.,[44] where

$$\langle \nu l | r | \nu' l' \rangle = \{(3/2)\nu_c{}^2 [1-(l_c/\nu_c)^2]^{1/2}\} \sum_{p=0,3} \gamma^p g_p(s) \quad (9)$$

with $\gamma = \Delta l(l_c/\nu_c)$, $s = \nu - \nu'$, $l_c = \max(l,l')$, $\Delta l = l' - l$, and $\nu_c = 2/(1/\nu + 1/\nu')$. The functions $g_p(s)$ are given in ref 44.

In the Stark Hamiltonian used in the calculations in this paper all the angular momentum states $l = 0, ..., n-1$ ($4n-2$ levels for each value of the principal quantum number) were included for a particular value of the principal quantum number. Calculations to determine the properties of the Rydberg series for the principal quantum number of interest were performed over an energy range, which included levels with (effective) principal quantum number $n-1$, n, and $n+1$. Therefore the calculations at $n = 60$ involve a diagonalization of (714×714) matrices.

(b) Calculation of Experimental Observables. By diagonalization of the Stark Hamiltonian (eq 1) the eigenvalues of the Stark states are obtained, as well as expressions for the eigenvectors of these states in terms of the field-free basis states:

$$|i\rangle_{\text{Stark}} = \sum_{\alpha} A_{i\alpha} |\alpha\rangle_{nlKJ} \quad (10)$$

Using the expressions for the eigenvectors, the decay rate of the Stark states is calculated as a weighted sum of the decay rates of the basis states contributing to the Stark states:[39]

$$\Gamma_{i,\text{Stark}} = \sum_{\alpha} |A_{i\alpha}|^2 \Gamma_{\alpha} \quad (11)$$

The measured pulsed field ionization (PFI) signal depends on the central laser excitation frequency ω_{laser} and the time delay Δt between the laser excitation and the switching of the field excitation pulse and is approximated as

$$S(\omega_{\text{laser}},\Delta t) = \sum_i |A_{i\alpha 0}|^2 \exp(-2\pi \Delta t/h\Gamma_i) / \int d\omega' \times$$
$$\Gamma_i^{-1}[1+(\omega_i-\omega')^2/\Gamma_i^2]^{-1} \exp[-(\omega'-\omega_{\text{laser}})^2/\Delta\omega_{\text{laser}}{}^2] \quad (12)$$

where $|\alpha_0\rangle$ represents the zero-order basis state (ns′$[1/2]_1$ or nd′-$[3/2]_1$) which is responsible for the absorption. Similar to eq 15 in our paper on NO,[29] the PFI signal at a given time delay is calculated as an incoherent sum over Stark states, where the contribution of a given Stark state depends on the overlap of the Stark state with the zero-order state, the overlap between the absorption line and the laser bandwidth, and the lifetime of the individual Stark state. A difference compared to the expression used in ref 29, is that the overlap between the absorption lines and the laser bandwidth is calculated as a convolution integral between a Lorentzian absorption line profile and a Gaussian laser profile (in ref 29 the former had been neglected). We will briefly return to the issue of coherent versus incoherent detection of Rydberg states in the Discussion section.

Results

In Figure 1 a number of absorption spectra are presented in the vicinity of the 60s′$[1/2]_1$ level, which were obtained under four different conditions. The spectra were calculated by adding the contributions from both excitation to ns′$[1/2]_1$ and nd′$[3/2]_1$ orbitals. These contributions were weighed in a ratio of 1:12.8, which is the ratio of the integrated peaks corresponding to ns′$[1/2]_1$ and nd′$[3/2]_1$ in the experimental total ion yield spectra at zero field.[14] We note that the hyperfine structure which was experimentally observed in ref 14 is not included in the calculations. In the calculations of Figure 1a,c the dc electric field was zero, whereas in Figure 1b,d the field was equal to 2.5 V/cm, leading to the observation of resolvable Stark structure in the spectra (similar to the experiments, a 0.005 cm^{-1} laser bandwidth was employed in the calculations). Furthermore, in Figure 1a,b the s′/d′ mixing angle describing short-range Rydberg electron−core interactions was equal to zero, whereas in Figure 1c,d the angle was set to 0.15 radians. At this mixing angle the state termed ns′$[1/2]_1$ contains 98% $l = 0$, and 2% $l = 2$, as was the case in the analysis by Lu.[43] A comparison of the spectra of parts a and b, with respect to parts c and d of Figure 1 shows that the short-range core interactions induce hardly any changes in the intensity distributions in the absorption spectra.

The short-range core interactions do however strongly influence the ensuing *dynamics* of the Rydberg states. In Figure 2 the dependence of the PFI signal on the dc electric field is shown for three values of the s′/d′ mixing angle at the peak corresponding to the 60s′$[1/2]_1$ level. The calculations were carried out at a time delay of 3.2 ns, where, without dc electric field, the signal has dropped to approximately 5% of the signal calculated at zero time delay. We note that, except at very small time delays, the peaked structure in the curves shown in Figure 2 is not overly sensitive to the particular choice of the time delay. At short time delays the dc electric field dependence of the PFI signal relates to the field dependence of the absorption spectrum, whereas at later times, the field dependence of the PFI signal reflects field-induced changes to the lifetimes of the excited Rydberg state due to *l*-mixing. The experiments that we seek to explain were done at a PFI time delay where the PFI signal measured at zero field could be enhanced almost 20-fold by the application of a dc field (see Figure 5). This is the reason that the data in Figure 2 are presented for a time delay where at zero field about 95% of the initial population has decayed. The data in Figure 2 show that in the absence of s′/d′ mixing, the decay of the 60s′$[1/2]_1$ state is virtually independent of the dc electric field, as long as the field is below 0.5 V/cm. Only for a few isolated electric field strengths does an appreciable Rydberg population persist at the chosen time delay, while for most field strengths the Rydberg population decays at a rate that is near the field-free decay rate. A substantial enhancement beyond the natural decay rate due to *l*-mixing is seen at field strengths above 0.65 V/cm.

The situation is radically different when s′/d′ mixing is included in the calculations. As observed in Figure 2b,c, the onset for lifetime enhancement due to *l*-mixing comes at significantly lower field strengths when s′/d′ mixing is included. Both in Figure 2b, for a mixing angle of 0.075 radians, and in Figure 2c, for a mixing angle of 0.15 radians, the lifetime is enhanced as soon as a dc field in excess of 50 mV/cm is applied. Starting from these field strengths, the decay rates stay below the natural decay rate over a wide range of field strengths. As in the calculation of Figure 2a without s′/d′ mixing, extensive resonance structures are seen. However the important difference with Figure 2a is that the resonance structures become important at a significantly *lower* field strength and, furthermore, that the lifetime is enhanced over a wider range of dc electric field strengths.

The differences between part a and parts b,c in Figure 2 can be traced to the appearance of the Stark map of the Xe atom.

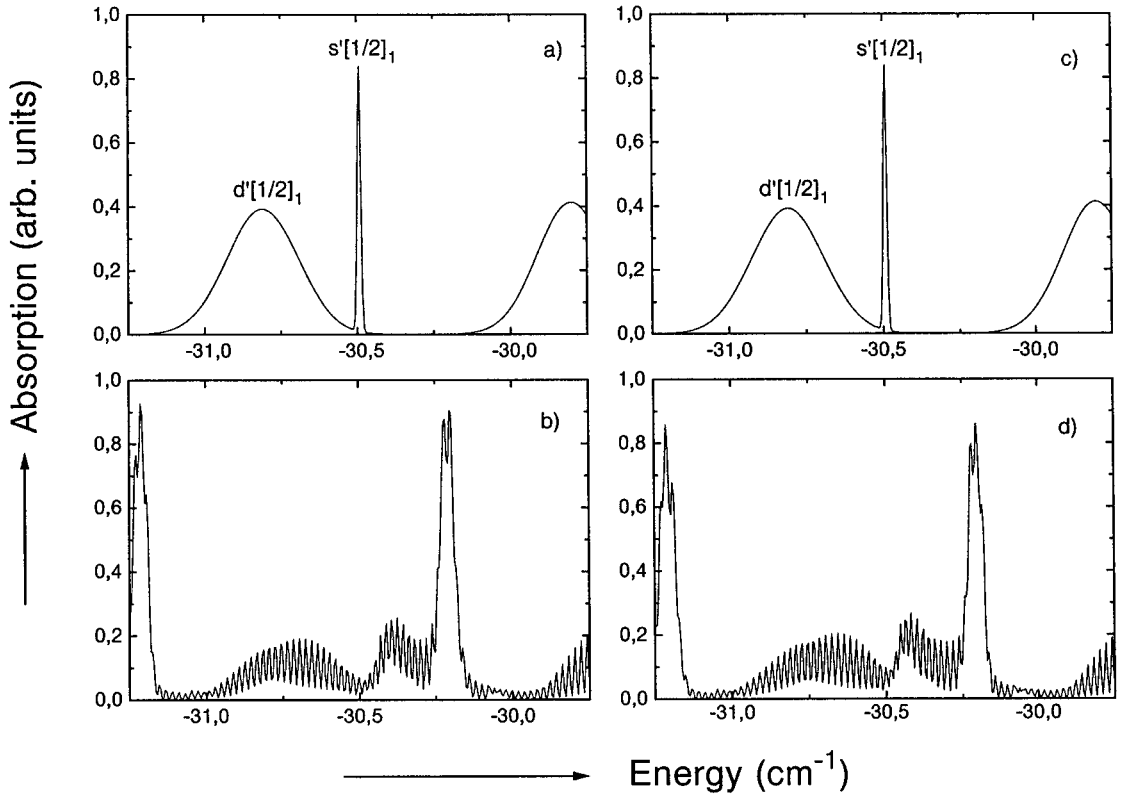

Figure 1. Xe excitation spectra calculated in the vicinity of the 60s′[1/2]$_1$ level, calculated under the following conditions: (a) 0 V/cm; 0 radian s′/d′ mixing angle; (b) 2.5 V/cm; 0 radian s′/d′ mixing angle; (c) 0 V/cm; 0.15 radians s′/d′ mixing angle; (d) 2.5 V/cm; 0.15 radians s′/d′ mixing angle.

In a Stark map the location of Rydberg energy levels is shown as a function of the dc electric field strength. As shown in Figure 3, where a Stark map in the vicinity of the 40s′[1/2]$_1$ level is presented, the ns′[1/2]$_1$ level undergoes a number of avoided crossings with a hydrogenic manifold which is formed from the high-l ($l > 3$) states. These high-l states have zero quantum defect at zero field. The onset for the crossings between the ns′[1/2]$_1$ level and the high-l states occurs at a very small field, since the reduced quantum defect of the ns′[1/2]$_1$ series is only 0.01. This means that at zero field the energy difference between the ns′[1/2]$_1$ levels and the high angular momentum states is very small (only 5×10^{-3} cm^{-1} at $n = 60$). The first crossing comes when the halfwidth of the Stark manifold $(3/2)Fn^2$ becomes comparable to the zero-field offset μ/n^3 between the 60s′[1/2]$_1$ state and the high-l manifold. Using a quantum defect for the 60s′[1/2]$_1$ of 0.010, it follows that the first crossing of the 60s′[1/2]$_1$ level with the Stark manifold takes place at a field strength of 44 mV/cm, which is exactly where the changes in the lifetimes first appear. In the calculations without s′/d′ mixing the influence of the avoided crossings does not manifest itself in the electric field dependence of the PFI signal until the field reaches a strength of approximately 0.50 V/cm, where the resonances begin to extend over a wider range of electric field strengths and a measurable lifetime enhancement takes place.

The reason for the lifetime enhancement is further illustrated in Figure 4. An enlargement of the encircled portion of the $n = 40$ Stark map of Figure 3 is shown, for an s′/d′ mixing angle of 0 radians (Figure 4a) and 0.15 radians (Figure 4b). The s′/d′ core mixing makes the crossings between the ns′[1/2]$_1$ state and the high-l manifold considerably more avoided. Two adiabatic eigenstates are formed, which are a mixture of the diabatic states that participate in the crossing (the ns′[1/2]$_1$ level and one of the high-l-mixed Stark states). The amount of mixing that takes place and the width ΔF over which the mixing manifests itself are determined by the strength of the coupling between the two diabatic states. Since the high-l-mixed Stark states couple with the diabatic ns′[1/2]$_1$ states subject to the selection rule $\Delta l = \pm 1$, the coupling will be determined to a large extent by the amount of d′[3/2]$_1$ character that the ns′[1/2]$_1$ state has acquired through the short-range Rydberg electron−core interactions. It is in this fashion that short-range core interactions become a major factor in determining the electric field dependence of the experimental pulsed field ionization signals: s′/d′ mixing provides a route for the ns′[1/2]$_1$ level to couple to the high-l manifold, well before the Stark states acquire large amounts of d′ character.

Comparison with Experimental Results and Discussion

In Figure 5 experimental results of the dc electric field dependence of Xe 60s′[1/2]$_1$ PFI signals are reproduced, which were recorded at a pulsed field time delay of about 80 ns. The experimental results are compared to results of our theoretical calculations which were obtained with an s′/d′ mixing angle of 0 radians (Figure 2a) and 0.15 radians (Figure 2c). For convenience, in Figure 5 the oscillatory resonance structures in Figure 2a,c have been smoothed by integrating the curves of Figure 2 within bins with a width of 0.025 V/cm. It is clear from Figure 5 that the rapid increase of the PFI signal at low field which is seen in the experimental data can only be reproduced when s′/d′ mixing is included in the calculations. While in the calculation including s′/d′ mixing the onset for the lifetime enhancement of the Rydberg states comes at a field strength of only 50 mV/cm (determined by the quantum defect of the s′[1/2]$_1$ series), in the calculation without s′/d′ mixing the onset for lifetime enhancement comes at fields in excess of 0.5 V/cm. We note that for the d′[3/2]$_1$ series the first crossing with the high-l manifold is reached at a field strength of approximately 1.35 V/cm, at which point a decay of the ns′[1/

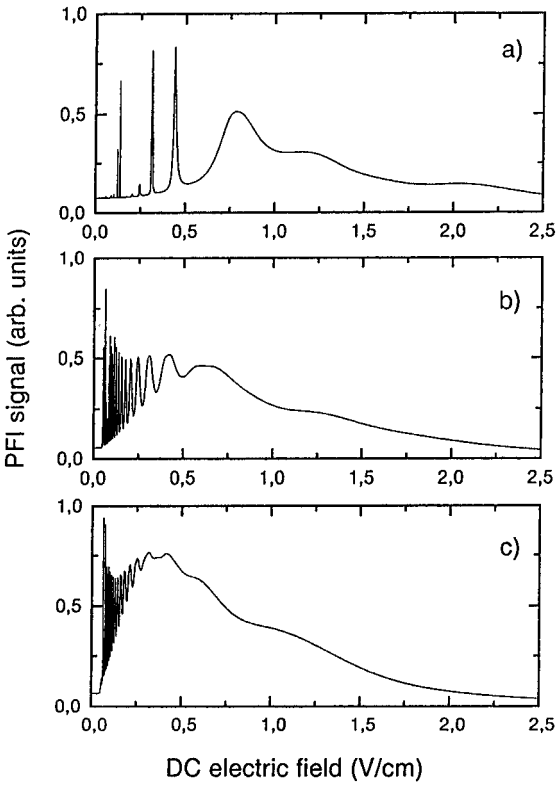

Figure 2. Calculated PFI signals as a function of the existing dc field at a time delay of 3.2 ns, following excitation at the 60s′$[1/2]_1$ peak. The calculations were performed for three values of the s′/d′ mixing angle, namely, (a) 0 radians, (b) 0.075 radians, and (c) 0.15 radians. The inclusion of a nonzero s′/d′ mixing angle leads to significant interactions of the 60s′$[1/2]_1$ level with the nearby Stark manifold, prior to coupling of the 60d'$[3/2]_1$ level with this manifold.

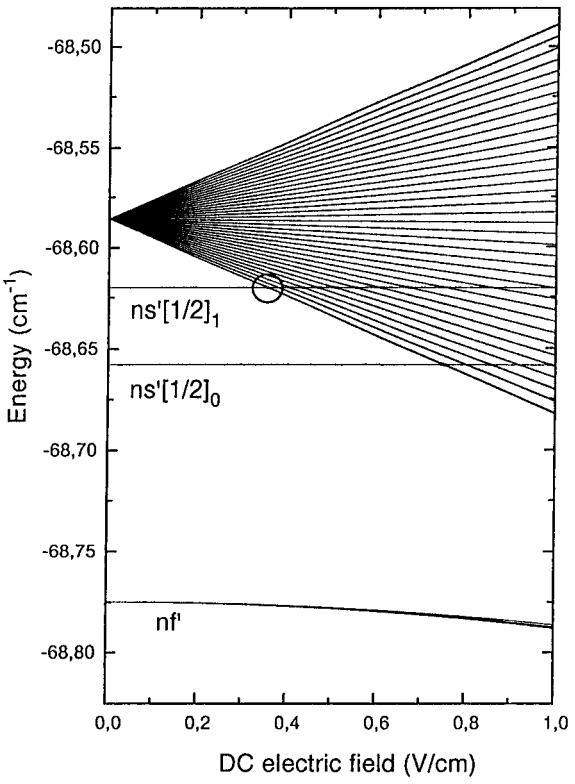

Figure 3. Xe Stark map calculated in the vicinity of the $n = 40$ high-l manifold, calculated without s′/d′ mixing. In order to calculate this Stark map, all levels with effective principal quantum number $n = 39-41$ were included in the matrix diagonalization. The Stark map shows the onset of crossings of the 40s′$[1/2]_1$ state with the high-l manifold near a field strength of 0.37 V/cm (encircled). Detailed calculations for this region with and without s′/d′ mixing are shown in Figure 4.

$2]_1$ PFI signal is observed in both the simulations and the experimental data. In conclusion, we observe that the onset of efficient l-mixing, as observed through changes in the lifetimes of the Rydberg states, is not hierarchical, but rather, that mixing of the 60s′$[1/2]_1$ state with the high-l manifold significantly precedes mixing of the 60d′$[3/2]_1$ state with the manifold. As demonstrated above, this is a manifestation of the fact that the ns′$[1/2]_1$ and nd′$[3/2]_1$ are coupled by a short-range Rydberg electron−core interaction, as a result of which the coupling of the ns′$[1/2]_1$ series to the high-l manifold is mediated by the nd′$[3/2]_1$ series.

Under the experimental conditions of the measurements in Figure 5 the PFI signals measured decayed with a time constant of approximately 50 ns, which exceeds the lifetimes calculated in the previous section by more than 1 order of magnitude. This is caused by the fact that the Xe Rydberg states that were field-ionized in the experiment not only had undergone a lifetime enhancement due to l-mixing but had also undergone m-mixing due to the presence of surrounding ions. In the experiment direct evidence for this mechanism involving a binary Xe−Xe interaction was obtained from the fact that the Xe PFI signal displayed a near-quadratic dependence on the Xe pressure. The presence of ions near the Rydberg atom, adds both a dc and an ac component to the electric field experienced by the atom. To the extent that the Rydberg atom and the ion are stationary with respect to each other, the additional field is dc, and the total field experienced by the atom is the vector sum of the externally applied dc field and the field due to the presence of the ion. Relative motion of the Rydberg atom and the ion leads to an AC component. The presence of the ions is relevant to our discussion in two ways. First of all, the added inhomogenous and time-dependent field components lead to m-mixing and an additional lifetime enhancement beyond the lifetime enhancement that we have calculated. Secondly, the dc component will lead to a smearing of the resonance structure in the calculated electric field dependence of the PFI signal, since experimentally we cannot control the Rydberg atom−ion internuclear distance. The experiments were carried out over an estimated range of ion densities from 10^5 to 10^7 ions/cm^3, corresponding to a median Rydberg atom−ion internuclear distance of 210−46 μm. At these internuclear distances the dc field contributed by the ion−Rydberg interactions is 0.3 and 6.8 mV/cm, respectively. These field strengths are comparable to the widths and spacings between the resonance structures observed in Figure 3, which accordingly are not observed in the experiment.

At the end of this paper, it is interesting to return briefly to the issue of coherent versus noncoherent detection of Rydberg states. In general, if Fourier-transform-limited laser pulses are used to excite a superposition of eigenstates, then the levels will be formed in a coherent superposition state, which will dephase and rephase on a time scale related to the inverse line spacing between the eigenstates in the superposition. In the current experiment, if a coherent superposition of Stark levels is populated, this coherent superposition will oscillate between low-l and high-l on a time scale given by $\tau_{\text{recurrence}} = (1/3)Fn$ (since the level spacing between adjacent Stark levels in a hydrogenic Stark manifold is equal to $3Fn$). As a consequence, the population will not undergo a single-exponential or even multiexponential decay, but rather, the decay rate should be oscillatory in time: autoionization is only expected at those times when the expectation value of the orbital angular momentum is small. The Xe pulsed field ionization experiments discussed here involved a mechanism where the magnetic

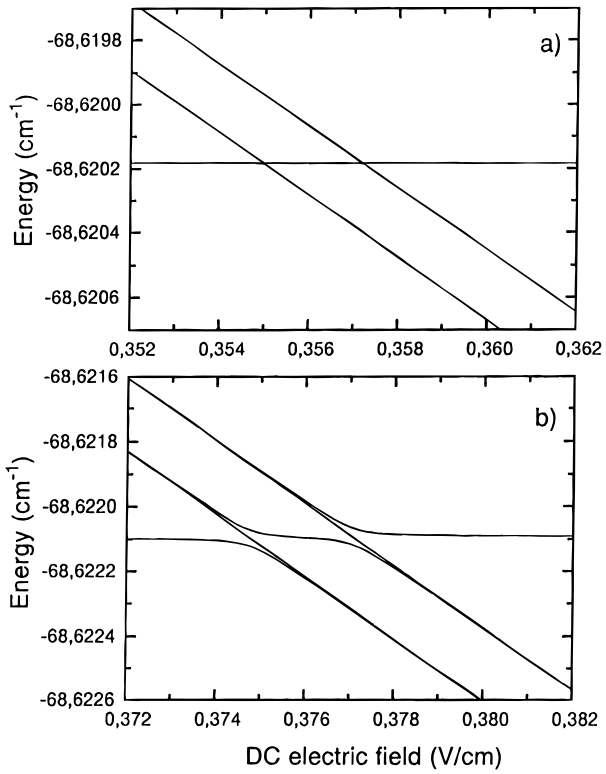

Figure 4. Detail of the Stark map of Figure 4, calculated with a s′/d′ mixing angle of (a) 0 radians and (b) 0.15 radians. The s′/d′ mixing leads to a significantly enhanced interaction (and an avoided crossing) between the diabatic 40s′$[1/2]_1$ state and members of the Stark manifold. Adiabatic states are formed in which the 40s′$[1/2]_1$ character and the high-*l* character is more thoroughly mixed than in the absence of s′/d′ mixing.

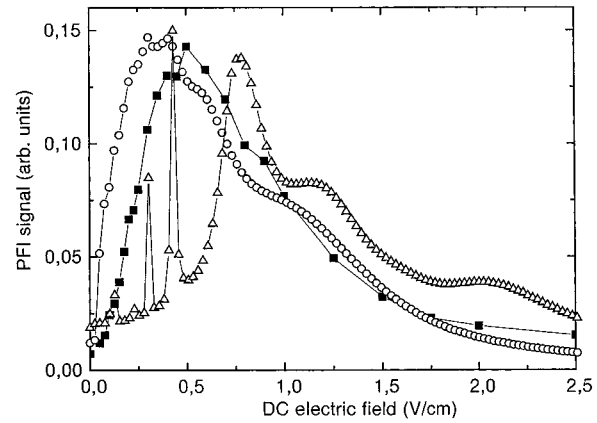

Figure 5. Comparison of the experimental dc electric field dependence of the PFI signal (solid squares), measured at a PFI time delay of 80 ns, to calculated results at a time delay of 3.2 ns, obtained using an s′/d′ mixing angle of 0 radians (open triangles) and 0.15 radians (open circles). The theoretical results were obtained by smoothing the calculated results shown in Figure 2a,c, by integrating the calculated curves within 0.025 V/cm bins.

quantum number was altered due to an inhomogeneous interaction with surrounding ions. Therefore, this is an incoherent experiment, and no oscillations were seen. With the development of an atomic streak camera[45] it has recently become possible to look at time-resolved ionization with (sub-) picosecond time resolution. It will be very interesting to study the dynamics of Xe autoionization at lower values of the principal quantum number ($n \approx 10$) in the time domain using picosecond laser excitation. In this regime it will be possible to study the effect of a dc electric field in a regime where surrounding ions will not have any effect. As a function of the applied dc electric field, we anticipate a transition from single-exponential decay at low field (excitation of low-*l* eigenstate) to oscillatory behavior once the low-*l* state has been absorbed into the Stark manifold. Of particular interest is excitation near one of the crossings in the Stark map, where one can tune the dc electric field onto the avoided crossing and where the time scale of an anticipated quantum beat provides direct information on the coupling between the diabatic states at the crossing and, hence, the extent of Rydberg electron−core induced mixing between the ns′$[1/2]_1$ and nd′$[3/2]_1$ series.

Acknowledgment. I am greatly indebted to Prof. Yuan Lee, who provided a wonderful and stimulating scientific training ground to his graduate students and postdocs in Berkeley, and in whose laboratory the experiments that motivated this paper were carried out. I further especially want to acknowledge Prof. Bill Chupka, who first drew my attention to the possible importance of the short-range interactions that form the subject of this paper. I would like to acknowledge Profs. Turgay Uzer, Frederic Merkt, Hans-Jurgen Neusser, Edward Schlag, and John Hepburn for making references 13, 18, 20, 22, and 24 available prior to publication. The Royal Dutch Academy of Sciences (KNAW) is acknowledged for receipt of an Academy Fellowship. This work is part of the research program of the "Stichting voor Fundamenteel Onderzoek der Materie (FOM)", which is financially supported by the "Nederlandse organisatie voor Wetenschappelijk Onderzoek (NWO)".

References and Notes

(1) Vrakking, M. J. J.; Lee, Y. T. *Phys. Rev. A* **1995**, *51*, R894.
(2) Vrakking, M. J. J.; Lee, Y. T. *J. Chem. Phys.* **1995**, *102*, 8818.
(3) Rabani, E.; Levine, R. D.; Even, U. *J. Phys. Chem.* **1994**, *98*, 8834.
(4) Rabani, E.; Levine, R. D.; Muhlpfordt, A.; Even, U. *J. Chem. Phys.* **1994**, *102*, 1619.
(5) Remacle, F.; Levine, R. D. *J. Chem. Phys.* **1996**, *104*, 1399.
(6) Remacle, F.; Levine, R. D. *J. Chem. Phys.* **1996**, *105*, 4649.
(7) Chupka, W. A. *J. Chem. Phys.* **1993**, *99*, 5800.
(8) Chupka, W. A. *J. Chem. Phys*. **1993**, *98*, 4520.
(9) ten Wolde, A.; Noordam, L. D.; Lagendijk, A.; van Linden, H. B.; Heuvell, van den *Phys. Rev. A* **1989**, *40*, 485.
(10) Bordas, C.; Brevet, P. F.; Broyer, M.; Chevaleyre, J.; Labastie, P.; Perrot, J. P. *Phys. Rev. Lett.* **1988**, *60*, 917.
(11) Rabani, E.; Baranov, L. Ya.; Levine, R. D.; Even, U. *Chem. Phys. Lett*. **1994**, *221*, 473.
(12) Held, A.; Baranov, L. Ya.; Selzle, H. L.; Schlag, E. W. *Z. Naturforsch*. **1996**, *51a*, 1236.
(13) Bellomo, P.; Farrelly, D.; Uzer, T. Submitted for publication.
(14) Vrakking, M. J. J.; Lee, Y. T. *J. Chem. Phys.* **1995**, *102*, 8833.
(15) Pratt, S. T. *J. Chem. Phys.* **1993**, *98*, 9241.
(16) Merkt, F. *J. Chem. Phys.* **1994**, *100*, 2623.
(17) Merkt, F.; Zare, R. N. *J. Chem. Phys.* **1994**, *101*, 3495.
(18) Palm, H.; Merkt, F. *Chem. Phys. Lett.* **1997**, *270*, 1.
(19) Neuhauser, R.; Neusser, H. J. *Chem. Phys. Lett.* **1996**, *253*, 151.
(20) Neuhauser, R. G.; Siglow, K.; Neusser, H. J. *J. Chem. Phys.* **1997**, *106*, 896.
(21) Held, A.; Selzle, H. L.; Schlag, E. W. *J. Phys. Chem.* **1996**, *100*, 15314.
(22) Held, A.; Selzle, H. L.; Schlag, E. W. *Chem. Phys. Lett.*, accepted for publication.
(23) Alt, C.; Scherzer, W. G.; Selzle, H. L.; Schlag, E. W. *Chem. Phys. Lett.* **1995**, *240*, 457.
(24) Martin, J. D. D.; Alcaraz, C.; Hepburn, J. W. *J. Phys. Chem.* **1997**, *101*, 6728.
(25) Hsu, C.-W.; Lu, K. T.; Evans, M.; Chen, Y. J.; Ng, C. Y.; Heimann, P. *J. Chem. Phys.* **1996**, *105*, 3950.
(26) Merkt, F.; Xu, H.; Zare, R. N. *J. Chem. Phys.* **1996**, *104*, 950.
(27) Xu, H.; Shafer-Ray, N. E.; Merkt, F.; Hughes, D. J.; Springer, M.; Tuckett, R. P.; Zare, R.N. *J. Chem. Phys.* **1995**, *103*, 5157.
(28) Vrakking, M. J. J.; Fischer, I.; Villeneuve, D. M.; Stolow, A. *J. Chem. Phys.* **1995**, *103*, 4538.
(29) Vrakking, M. J. J. *J. Chem. Phys.* **1996**, *105*, 7336.
(30) Jortner, J.; Bixon, M. *J. Chem. Phys.* **1995**, *102*, 5636.
(31) Bixon, M.; Jortner, J. *J. Phys. Chem.* **1995**, *99*, 7466.

(32) Wales, N. P. L.; Buma, W. J.; de Lange, C. A.; Lefebvre-Brion, H. *J. Chem. Phys.* **1996**, *105*, 5702.
(33) Fano, U. Phys. Rev. A **1970**, *2*, 353.
(34) Greene, C. H.; Jungen, Ch. *Adv. Atom. Mol. Phys*. **1985**, *21*, 51.
(35) Fredin, S.; Gauyacq, D.; Horani, M.; Jungen, C.; Lefebvre, G. *Mol. Phys.* **1987**, *60*, 825.
(36) Bixon, M.; Jortner, J. *J. Chem. Phys.* **1996**, *105*, 1363.
(37) Softley, T. P.; Hudson, A. J.; Watson, R. *J. Chem. Phys.* **1997**, *106*, 1041.
(38) Knight, R. D.; Wang, L.-G. *Phys. Rev. A* **1985**, *32*, 896.
(39) Ernst, W. E.; Softley, T. P.; Zare, R. N. *Phys. Rev. A* **1988**, *37*, 4172.
(40) Bixon, M.; Jortner, J. *J. Chem. Phys.* **1995**, *103*, 4431.
(41) Bixon, M.; Jortner, J. *J. Chem. Phys.* **1996**, *105*, 1363.
(42) Wang, L.-G.; Knight, R. D. *Phys. Rev. A* **1986**, *34*, 3902.
(43) Lu, K. T. *Phys. Rev. A* **1971**, *4*, 579.
(44) Edmonds, A. R.; Picart, J.; Tran Minh, N.; Pullen, R. *J. Phys. B* **1979**, *12*, 2781.
(45) Lankhuijzen, G. M.; Noordam, L. D. *Opt. Commun*. **1996**, *129*, 361.